Historical carpentry corner log joints—Numerical analysis within stochastic framework

Paweł Kłosowski, Izabela Lubowiecka*, Anna Pestka, Katarzyna Szepietowska

Gdańsk University of Technology, Faculty of Civil and Environmental Engineering, Department of Structural Mechanics, ul. Narutowicza 11/12, 80-233 Gdańsk, Poland

ABSTRACT

The paper presents the results of numerical analysis performed on historical, traditional carpentry corner log joints of two basic topologies: the short-corner dovetail connection and the saddle notch connection. These types of carpentry joints are commonly used in currently preserved objects of wooden architecture. All connections have been modelled in pinewood, which has been defined in the Finite Element software MSC.Marc/Mentat as an orthotropic material. The numerical calculations have been carried out for two types of connections with two different boundary conditions and load types. The contact phenomenon between the individual elements of the connections has been taken into account. The main purpose of the research is to select the most damage-resistant type of connection and to determine the stress distributions on the contact surfaces, which demines the damage areas. However, a lot of uncertainties appear in the studied models, e.g. due to the natural variability of the material properties of wood and the uncertainty of friction coefficient. Therefore the uncertainty quantification and global sensitivity analysis has been performed in order to include these uncertainties and study their effect on variation of the mechanical response of the connections. A regression-based non-intrusive polynomial chaos expansion method has been employed to complete the task.

The state-of-the-art knowledge about the damage-prone zones in the considered connections is immensely important since many wooden buildings, mostly historical, require maintenance, renovation and the reinforcement of existing, especially historical elements. On the contrary, there are not many results of related research published yet.

1. Introduction

Formerly, wood was extensively used in the structural engineering due to good strength parameters and a wide accessibility of the material. In civil engineering, concrete and steel are still more widespread structural materials than wood, which is more complicated in analysis and design due to its heterogeneity and the lack of isotropy. Wood defects such as knots, slope of grain, shake decay, burls, defects caused by fungi, stains and rots, and defects due to insects are often additional reasons for this heterogeneity [1]. As a natural material, wood is highly sensitive to moisture and damage by biological agents [2,3], its limits in terms of strength and elasticity depend primarily on humidity, temperature, density and aging [4]. All these impacts result in high variability of material properties of wood. In recent years a general awareness has grown with regard to the necessity of rehabilitating historic buildings especially of a heritage value. Due to economic and cultural factors nowadays, more attention is focused on the rehabilitation and restoration of old structures and on decreasing the

level of waste [5]. A reliable structural analysis leads to an efficient repair or supports solutions necessary to ensure the safety of the structure, thus it must be based on relevant modelling of the material, the joints and the entire structure.

Many types of carpentry joints can be distinguished with respect to their form and expected function [6]. A number of research works focusing on carpentry joints have been published recently, especially on joints in pieces at an angle, such as the birdsmouth joint in rafter to tie beam joints, the mortise and tenon joint, scarf joint, dovetail joint, as well as joints where the members are connected by their ends to achieve greater lengths (e.g., [7,8]). But the vast majority of research on carpentry connections concern analysis of typical joinery in the historic roof structures using monotonic tests [9], photo-elasticity tests and numerical analysis (see e.g., [10,11]). An approach taking into account the effect of temperature and humidity on the strength of wood is presented in [12–14]. Also a stress distributions and failure analysis of timber structures [15,16] as well as some experimental [17,18] and numerical [19–21] research are reported in the literature.

---

* Corresponding author.
  E-mail addresses: klosow@pg.edu.pl (P. Kłosowski), lubow@pg.edu.pl (I. Lubowiecka), annmlecz@pg.edu.pl (A. Pestka), katszepi@pg.edu.pl (K. Szepietowska).

The study is based on a probabilistic approach, which although having been used in the analysis of timber structures, is not yet used in simulations of corner log connection. One of the issues in numerical modelling of timber structures are uncertainties e.g. due to the natural variability of wood properties. The uncertainties of different sources can be included in models and design by means of random approach. It has been completed for design and robustness analysis of timber structures [22] and reliability analysis of old timber truss [23]. Non-intrusive probabilistic methods are based on a number of deterministic computations, to be employed in the "black-box" models created in commercial FE software. The Monte Carlo (MC) simulation method is a widely implemented non-intrusive method of uncertainty propagation in timber structures too [24]. Nevertheless, the method is computationally expensive since it requires a large number of simulations. In the case of complex FE models, triggering expenses to a single simulation the MC can be intractable. Some methods to reduce the computational cost of uncertainty propagation have been developed as presented in [25]. Kandler and Füssl [26] compared perturbation method and polynomial chaos expansion method with the MC and experimental results on the example of glue laminated timber. In order to investigate the effect of variation of each random variable on global uncertainty of the model response, sensitivity analysis methods can be employed. Sobol' indices [27] are widely-used global sensitivity measures. They have been used to study the importance of micromechanical parameters of wood on its macroscopic properties [28].

However, while applied mostly during past centuries in historical buildings, one can hardly find studies on carpentry joints related to corner joints of the solid walls in log-system buildings, where the joists are laid horizontally (see e.g., [29] or the Authors preliminary work [30]). Few, but interesting studies refer to the walls behaviour under seismic load and to the material modelling and experimentation [31,32]. The knowledge of the corner carpentry connections is enormously useful due to the necessary maintenance, renovation and the reinforcement of existing elements in many historical timber structures [33].

The development of carpentry, dated to the period from the 13th to 17th century, contributed to significant improvements in craft and techniques for making joints that allowed the use of a number of newly invented types of carpentry joints, and which modified those already known [34]. The modifications of the connections mainly consist of geometry variation and the introduction of locks inside the joint. The log buildings had hardly been the work of professional carpenters; they were rather constructed by the owners' families with the help of neighbours, there was an oral building tradition passing from one generation to another [29]. To this day, one wonders about the reason for constructing very complex connections, including hidden locks discovered during renovation and restoration [35].

The corner joints are essential parts of the structural system of the building, ensuring proper force transmission from external loads, as well as providing the spatial stiffness of the object. While conducting a 3D analysis of a corner joint, the distribution of internal forces is variable at the height of the wall, which is due to the dead load of the wall. In addition, the configuration of forces in the corner also depends on the architectural form of the building, including the roof systems, the thickness and slenderness of the walls and the technical state of the building.

The numerical modelling of the corner wall connection is a complex issue. The study presents models of historic carpentry corner log joints of two basic topologies (see e.g., [32]): the short-corner dovetail joint and the saddle notch joint, using different boundary conditions and different load systems to perform the finite element analysis. The main goal of the study is to find the stress distribution in the loaded wall with traditional corner carpentry joints constructed from logs in different ways, to learn about their static behaviour, and thus provide the basis for their reliable rehabilitation. Moreover, due to the modelling uncertainties, a probabilistic approach has been employed. The polynomial chaos expansion (PC) method in a non-intrusive regression variant [36] has been employed to propagate the uncertainties. The Sobol' indices have been computed in order to study the influence of the input uncertainties on the variation of the response of the modelled joint. The sensitivity of mean and extreme values of principal stress has been studied in a chosen location in the corner carpentry joints on variations of the Young's modulus of wood and of its friction coefficient.

2. Material and methods

2.1. Geometry of carpentry joints and material parameters

The entirety of surviving connections in the authentic historical buildings shows the cases of various geometries of a given connection. They are usually affected by location and time of a structure erection. In the study, the geometry of the connections described by [37] has been assumed with dimensions scaled into 1:2. The scale 1:2 has been selected due to preparation for laboratory tests. Each analysed carpentry joint taken for the analysis consists of five logs. The cross-sectional dimensions of a single log are 75×135 mm. The length of each wooden beam is 1000 mm for the short-corner dovetail connection and 1075 mm for the carpentry joint with protrusions, the saddle notch joint. The geometry of each carpentry joint scheme is presented in Fig. 1.

It is assumed that all carpentry joints are made of pinewood, because this is one of the most widely-used kinds of wood in traditional timber houses in southern Poland and western Ukraine. Their material properties vary with the direction of fibres thus they are considered orthotropic. The anatomical directions in the wood can be distinguished according to the following three directions: R—radial direction, T—tangential direction and L—longitudinal direction to the surface of each layer of the fibres [38,30]. The Young's modulus along the fibres E_L has been determined on the basis of the 4-point bending tests. The scheme of the laboratory stand is presented in Fig. 2. Eight bending tests with the test velocity 0.05 mm/s has been performed. The values of the Young's modulus E_L, obtained from the tests are presented in Table 1.

Other moduli E_T, E_R, G_{RT}, G_{TL}, G_{LR} are related to the Young's modulus E_L (see Table 2). In turn the Poisson's ratios ν_{RT}, ν_{TL}, ν_{LR} are taken from the literature [1].
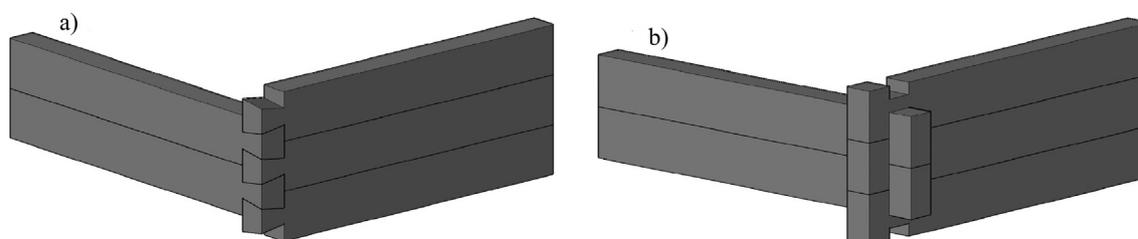

Fig. 1. Structure of corner log joints: (a) short-corner dovetail connection (Type 1), (b) saddle notch (Type 2).
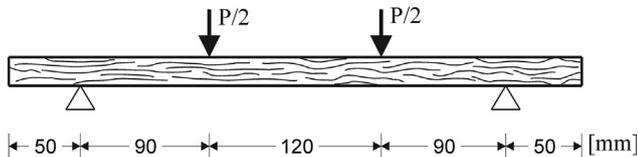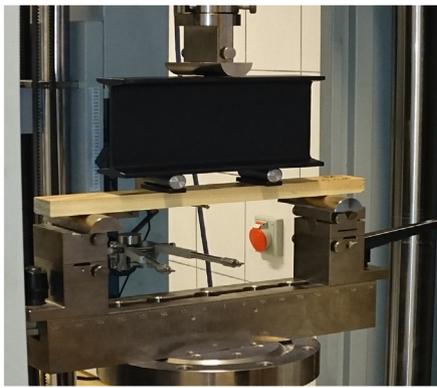
Table 2
Material parameters of pinewood [1].

E_T/E_L	E_R/E_L	G_{RT}/E_L	G_{TL}/E_L	G_{LR}/E_L	ν_{RT}	ν_{TL}	ν_{LR}
0.068	0.102	0.005	0.046	0.049	0.469	0.024	0.316

excessive deformations of wooden beams in the carpentry connections are very dangerous. The significant deformations of the logs cause high stresses on some contact surfaces. On the other hand, large displacements of logs expose the inside surfaces of the logs to environmental and biological degradation. The convergence analysis were conducted to assess the obtained FEM results. The h-type of the convergence was checked by refining the mesh twice. The mesh in the stress concentration area was refined at the stage of the model definition.

2.3. Random variables and quantities of interest in uncertainty propagation

The uncertainties of material properties of wood resulting from natural variability are high when compared to artificial construction materials like steel. Therefore, E_L expressed in [Pa] is assumed to be a log-normally distributed random variable $E_L \sim \mathcal{LN}(23.18, 0.23)$, following the recommendation in [39] with parameters adjusted to experimental results presented in Table 1. Other moduli vary together with E_L according to Table 2.

The wood-wood friction coefficient values, reported in literature vary significantly [40]. The friction coefficient between timber elements depends on moisture content, age, temperature, roughness and wood grain [41–43]. In the corner log joints the contribution of friction in its mechanical behaviour also depends on the initial gaps between logs (mounting tolerance), as shown in [32] where the Authors identified the friction coefficient in this type of corner joints and presented the interaction of friction and the interlock between logs. It certainly also depends on the surface of the contact area, so that on the joint geometry. But this aspect is not considered in our model. Due to lack of literature recommendation on the distribution of the friction coefficient and lack of own experimental studies, expert judgement approach is applied to choose uniform distribution in the reasonable approach. The friction coefficient μ is assumed here to be a uniformly distributed random variable $\mu \sim \mathcal{U}([0.1, 0.7])$. Necessity of proper identification of distributions will be shown by global sensitivity outcome.

The study is focused on the value of principal stress. Therefore, the mean of principal stress in chosen elements is the quantity of interest in uncertainty quantification and sensitivity analysis framework:

$$\bar{\sigma}_{max} = \frac{1}{n_{max}} \sum_{i=1}^{n_{max}} \sigma_{\max}^i, \tag{1}$$

$$\bar{\sigma}_{min} = \frac{1}{n_{min}} \sum_{i=1}^{n_{min}} \sigma_{\min}^i, \tag{2}$$

where $\sigma_{\max}^i$, $\sigma_{\min}^i$ are the maximum and minimum principal stress value at the integration point of *i*-th element from investigated set I_{max} and

Fig. 2. Laboratory stand and its scheme.

2.2. Finite element analysis

The numerical nonlinear static analysis with contact has been carried out using MSC.Marc Mentat software. The finite element method has been applied in modelling and in the analysis. The numerical model of each connection was defined using approximately 61,000 in case of dovetail and 101,000 in case of saddle notch three-dimensional tetrahedral solid elements. The discretisation of each connection model is more dense in the region of the analysed joint than in the rest of the log. The numerical calculation to determine the stress distributions have been performed for the mean value of Young's modulus E_L along a log presented in Table 1. Other moduli have been calculated in the relation to E_L on the basis of Table 2. The tangential direction modulus has been assumed to be parallel to Z global axis. The contact phenomenon has been defined between particular logs of the connections, assuming friction coefficient equal to 0.25. The numerical calculations have been performed with different boundary conditions of the carpentry joints in order to select the most resistant type of connection and to determine the stress distributions in the connection corners. For all carpentry joints, two variants A and B of boundary conditions and load cases have been carried out. The boundary conditions and load schemes applied in the Type 1 have been presented in two variants A and B (see Figs. 3 and 4, respectively). In both variants, the external surfaces of most bottoms of logs have been fixed in the direction Z. In turn, the Z translation of the top surfaces for most top logs has been fixed in the variant A, loaded with the pressure 10316.7 N/m² in the variant B. The pressure value has been assumed the wall dead load. It is made of nineteen logs lying above and distributed on the external surface of logs. The height of nineteen logs corresponds to the 2.5 m height of a structure wall. The

Table 1
Data from 4-point bending strength tests.

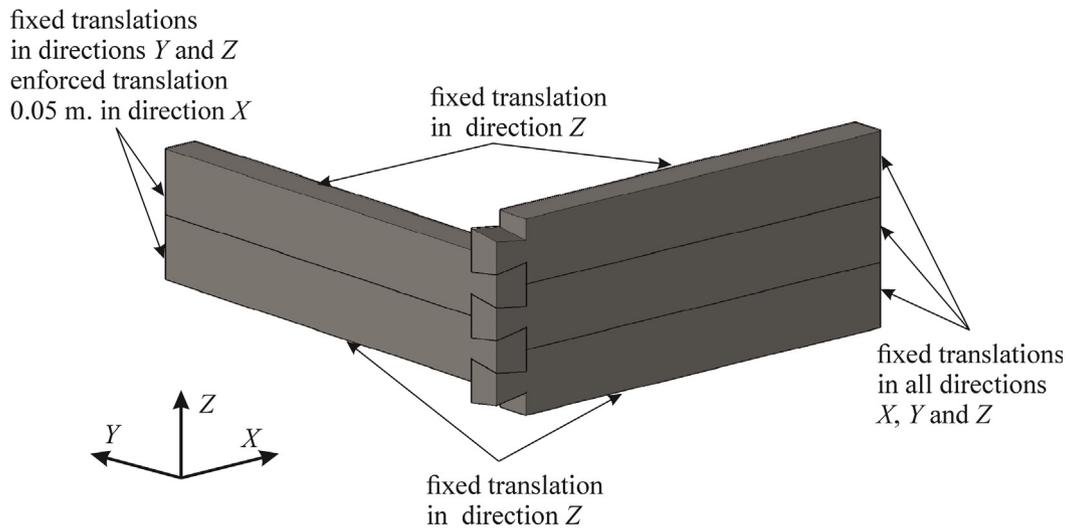| Specimen no.	Moisture content [%]	Cross-section [mm]	Length of specimen [mm]	Weight [g]	Density [kg/m³]	E_L [Pa]
1	7	39.7 × 19.8	400	168	534.3	1.44E+10
2	6.2	39.4 × 19.8	400	148	474.3	1.02E+10
3	7.2	39.3 × 19.9	400	167	533.8	1.19E+10
4	7.7	39.1 × 20.0	400	139	444.4	7.30E+09
5	8.7	39.5 × 19.7	400	185	594.4	1.46E+10
6	11.6	40.4 × 20.3	401	185	562.5	1.29E+10
7	12.6	39.9 × 20.0	402	171	533	1.36E+10
8	13.9	39.3 × 20.0	401	147	466.4	1.07E+10
					Mean	1.20E+10

Fig. 3. Boundary conditions applied in variant A.

I_{min} of n_{max} and n_{min} elements (Fig. 5), respectively. The chosen elements are located at the areas of high principal stress, which are subject of the research. The two types of joints have different geometry and work in a different way, so these areas are not exactly the same. Therefore, location and number of elements is also a bit different. However, the elements in case of both types are chosen following the same rule to find areas of high principal stresses. The additional quantity of interest is also the extremal principal stress in the chosen sets of elements:

$$\max\sigma_{max} = \max_{i\in I_{max}} \sigma_{max}^i \tag{3}$$

$$\min\sigma_{min} = \min_{i\in I_{min}} \sigma_{min}^i \tag{4}$$

The uncertainty quantification and global sensitivity analysis is performed only for variant A of boundary conditions. Variant A is chosen because the global sensitivity analysis is conducted here in order to draw conclusions relevant from the point of view of future experiment on carpentry joints, in which only forced displacement will be available to apply.

2.4. Polynomial chaos expansion method

The polynomial chaos expansion method (PC) is one of the stochastic spectral methods to reduce the number of simulations required for the uncertainty propagation. The method is based on the approximation of the model response by a series of multivariate polynomials. The following description of the PC method is based on [36,44].

Let $\mathcal{M}$ be a computational model, in the considered case one of the carpentry joint models. The inherent uncertainties lead to the introduction of the input random vector $\mathbf{X}(\omega)$ of a joint probability density function (PDF) $f_{\mathbf{x}}$ with the number of variables M, $\omega \in \Omega$, where Ω is the sample space consisting of elementary events ω. The random variables are assumed to be independent. In our case $\mathbf{X} = [E_L, \mu]^\top$. The output Y, a scalar, one of the defined quantities of interest (1)–(4) is consequently a random variable

$$Y(\omega) = \mathcal{M}(\mathbf{X}(\omega)) \tag{5}$$

In the following text ω is skipped for simplicity. In the PC method Y is expanded as follows:

$$Y = \sum_{\alpha\in\mathbb{N}^M} a_\alpha \Psi_\alpha(\xi), \tag{6}$$

where a_α are coefficients and ξ are reduced variables after the
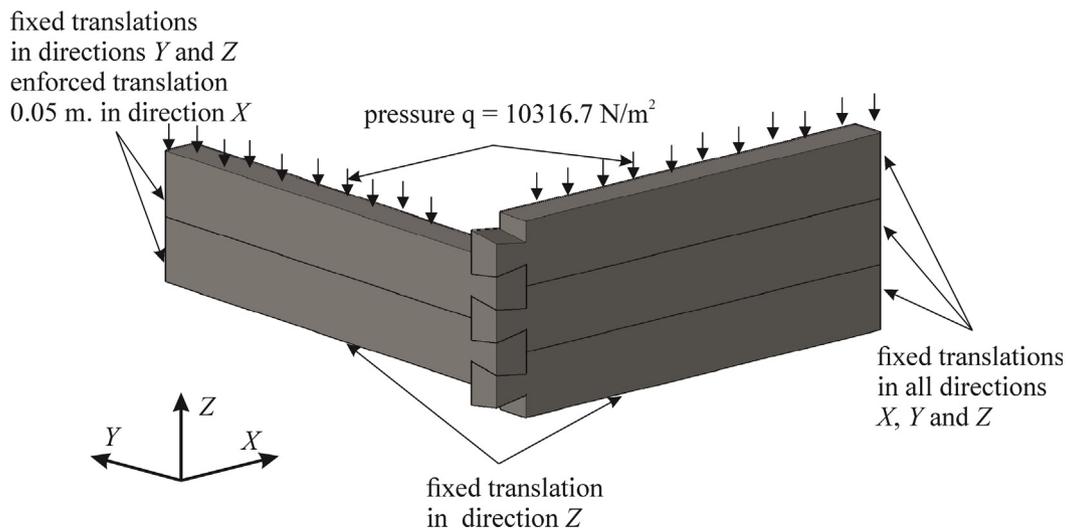

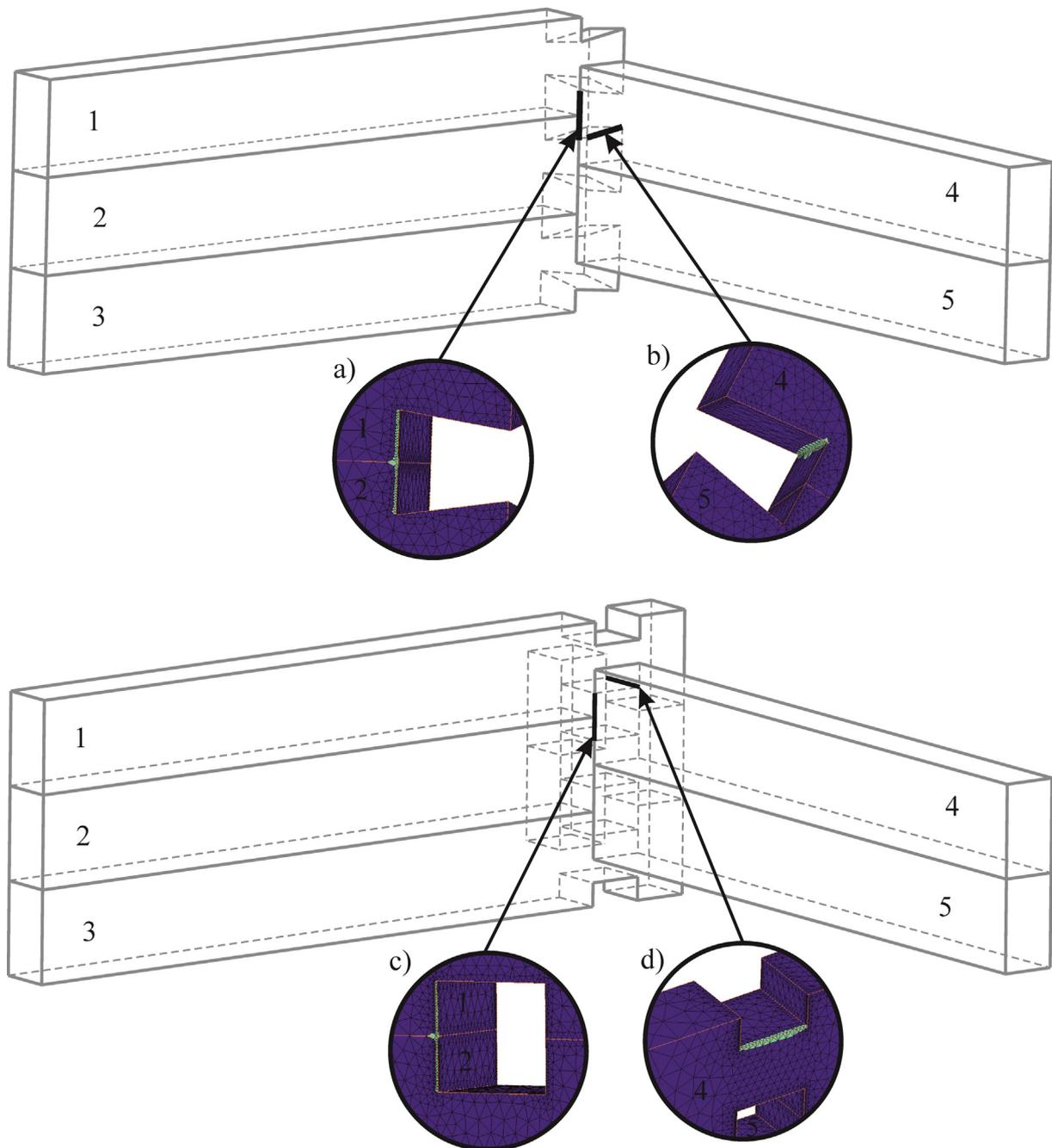Fig. 4. Boundary conditions applied in variant B.

Fig. 5. Investigated elements in uncertainty quantification framework: (a) I_{min} for dovetail joint, (b) I_{max} for dovetail joint, (c) I_{min} for saddle notch joint, (b) I_{max} for saddle notch joint.

isoprobabilistic transformation $\mathbf{X} = \mathcal{T}(\boldsymbol{\xi})$. A normal variable is transformed into the standard normal variable $\mathcal{N}(0, 1)$, the uniformly distributed variable is transformed into uniform $\mathcal{U}([-1, 1])$. Lognormal variable $X_i \sim \mathscr{LN}(\lambda, \zeta)$ can be transformed to standard normal variable $\xi_i \sim \mathcal{N}(0, 1)$

$$X_i = e^{\lambda + \zeta \xi_i}, \tag{7}$$

where λ and ζ are the mean and standard deviation of the variable's natural logarithm, respectively.

$\Psi_{\boldsymbol{\alpha}}$ is a multivariate polynomial basis, a multiplication of univariate polynomials $\Psi_{\boldsymbol{\alpha}} = \prod_{i=1}^{M} \psi_{\alpha_i}^{(i)}(\xi_i)$, α_i is the order of polynomial and $\boldsymbol{\alpha} = [\alpha_i, \ldots, \alpha_M]$ is a multi-index of orders of each univariate polynomials forming a multivariate polynomial.

The polynomials are orthonormal:

$$\langle \psi_i, \psi_j \rangle = \int \psi_i(\xi) \psi_j(\xi) f_\xi(\xi) d\xi = \delta_{ij}, \tag{8}$$

where δ_{ij} is the Kronecker delta. The Hermite polynomials are orthogonal with respect to Gaussian distribution measure and Legendre polynomials with respect to the uniform one. These sorts of polynomials are employed in the study. Infinite expansions need truncating in the analysis. A widely used method is to take all polynomials of the degree equal or smaller than a chosen degree p. In this case a truncation set is $\mathscr{A} = \{\boldsymbol{\alpha} \in \mathbb{N}^M : \sum_{i=1}^{M} \alpha_i \leqslant p\}$ and the final form of the PC approximation is:

$$Y \approx Y^{PC} = \sum_{\boldsymbol{\alpha} \in \mathscr{A}} a_{\boldsymbol{\alpha}} \Psi_{\boldsymbol{\alpha}}(\boldsymbol{\xi}). \tag{9}$$

A non-intrusive method to find the polynomial coefficients is the least-squares regression. The model $\mathcal{M}$ is applied on N regression points

$\Xi = [\boldsymbol{\xi}^{(1)}, ..., \boldsymbol{\xi}^{(N)}]$ and vector of exact solutions $Y_{ex} = [\mathscr{M}(\boldsymbol{\xi}^{(1)}), ..., \mathscr{M}(\boldsymbol{\xi}^{(N)})]^\top$ is created. The coefficients are arranged into a vector $\mathbf{a} = [a_{\alpha_0}, ..., a_{\alpha_{P-1}}]^\top$, where P is the cardinality of truncation set $\mathscr{A}$. The values of polynomials at the regression points are collected in a matrix $A_{ij} = \Psi_{\alpha_j}(\boldsymbol{\xi}^{(i)})$, where $i = 1, ..., N$ and $j = 1, ..., P$. The solution of the least square problem leads to

$$\mathbf{a} = (\mathbf{A}^\top\mathbf{A})^{-1}\mathbf{A}^\top Y_{ex}. \tag{10}$$

The matrix $\mathbf{A}^\top\mathbf{A}$ may be called an information matrix. The accuracy of the non-intrusive PC depends on the number and the choice of regression points. One of the approaches to choose points is to take the D-optimal points [45], which leads to the maximization of information matrix determinant. In the study, the D-optimal solution has been found from randomly chosen the candidate set of points following the Author's experience in regression points choice described in [46].

2.5. Global sensitivity analysis

The global sensitivity analysis allows to quantify the effect of uncertain inputs in the domain of their probability density function on the model output. The Sobol' indices [27] (following description based also on [44,47]) are based on the ANOVA (ANalysis Of VAriance) decomposition of the model response (5) as follows:

$$\mathscr{M}(\mathbf{X}) = \mathscr{M}_0 + \sum_{i=1}^{M} \mathscr{M}_i(X_i) + \sum_{1 \leqslant i < j \leqslant M} \mathscr{M}_{ij}(X_i, X_j) + \cdots + \mathscr{M}_{1,2...M}(\mathbf{X}), \tag{11}$$

and

$$\int_{\mathscr{H}_{X_k}} \mathscr{M}_{i_1...i_s}(X_{i_1}, ..., X_{i_s})f_{X_k}(X_k)dX_k = 0$$
$$\text{for} \quad 1 \leqslant i_1 < \cdots < i_s \leqslant M, \; k = i_1, ..., i_s \tag{12}$$

$$\mathscr{M}_0 = \int_{\mathscr{H}_{\mathbf{X}}} \mathscr{M}(\mathbf{X})f_{\mathbf{X}}(\mathbf{X})dX_i...dX_M, \tag{13}$$

where $\mathscr{H}_{\mathbf{X}}$ is the support of $\mathbf{X}$. $\mathscr{H}_{X_l}$ is the support and f_{X_k} is the PDF of the variable X_k, respectively. The Sobol' sensitivity index is defined as the ratio of variances:

$$S_{i_1, ..., i_s} = \frac{D_{i_1, ..., i_s}}{D}., \tag{14}$$

where $D_{i_1, ..., i_s}$ is a partial variance

$$D_{i_1...i_s} = \int_{\mathscr{H}_{X_{i_1}, ..., X_{i_s}}} \mathscr{M}_{i_1...i_s}^2(X_{i_1}, ..., X_{i_s})f_{X_{i_1}, ..., i_s}dX_{i_1}...dX_{i_s}, \tag{15}$$

and D a total variance

$$D = \int_{\mathscr{H}_{\mathbf{X}}} \mathscr{M}(\mathbf{X})^2 f_{\mathbf{X}} dX_1...dX_M - \mathscr{M}_0^2. \tag{16}$$

The total sensitivity index is defined as a sum of indices including the mixed terms

$$S_i^{Tot} = \sum_{i \subset \{i_1, ..., i_s\}} S_{i_1, ..., i_s}. \tag{17}$$

The computation of sensitivity indices can be provided analytically or by means of the MC. However, the MC variant is computationally expensive. Sudret [47] and Crestaux et al. [48] showed that due to the orthonormality of the PC basis the Sobol' indices can be computed using the PC coefficients without an additional computational cost. The Sobol' index can be calculated using the coefficients corresponding to multivariate polynomials containing given variables only:

$$S_{i_1, ..., i_s}^{PC} = \frac{1}{D^{PC}} \sum_{\boldsymbol{\alpha} \in \mathscr{A}_{i_1, ..., i_s}} a_{\boldsymbol{\alpha}}^2, \tag{18}$$

where $\mathscr{A}_{i_1, ..., i_s} = \{\boldsymbol{\alpha} \in \mathscr{A}: \alpha_k = 0 \Leftrightarrow k \notin \{i_1, ..., i_s\}\}$ and D^{PC} is the variance approximated by PC:

$$D \approx D^{PC} = \sum_{\boldsymbol{\alpha} \in \mathscr{A} \setminus \{\mathbf{0}\}} a_{\boldsymbol{\alpha}}^2. \tag{19}$$

The total Sobol' index can be obtained incorporating coefficients corresponding to polynomials containing given variables including mixed terms with other variables too:

$$S_i^{Tot,PC} = \frac{1}{D^{PC}} \sum_{\boldsymbol{\alpha} \in \mathscr{A}_i^{Tot}} a_{\boldsymbol{\alpha}}^2, \tag{20}$$

where $\mathscr{A}_i^{Tot} = \{\boldsymbol{\alpha} \in \mathscr{A}: \alpha_i > 0\}$.

3. Results

3.1. Results of deterministic analysis

The result comparison has been carried out for two carpentry connections taking into account different variants of boundary conditions presented in Figs. 3 and 4. The first insight into the analyzed connections shows there are slight differences between distributions of the minimum principal stress in variants A and B for the saddle notch joint. The specific stress distribution occurs in the short-corner dovetail connection. In the dovetail joint (Type 1), the highest stress values are concentrated only along the internal edges of the logs. For the saddle notch connection (Type 2) the high stress areas are larger than in the dovetail case (Figs. 6 and 7).

The short-corner dovetail connection shows an anti-symmetric distribution of the maximum and minimum principal stresses for the variant B in contrast to the symmetric stress distribution in the saddle notch joint of an identical boundary condition type (Figs. 6b–9b). The variant A shows that both connections exhibit symmetric stress distributions (Figs. 6a–9a). The high areas of the maximum principal stress are greater for the saddle notch than in the case of the dovetail connection. The maximum principal stress distributions in the corner of the saddle notch joint are almost identical for the variants A and B (Fig. 9). In turn, in the corner of the short-corner dovetail joint stress distribution are different, in the variant A the high stress areas are definitely greater than in the same connection for the variant B (Fig. 8).

3.2. Results of uncertainty quantification and global sensitivity analysis

Uncertainties are propagated by the PC method (3 order, 20 regression points) in the models of the variant A of loading. The obtained histograms of the quantities of interest $\overline{\sigma}_{max}$ and $\overline{\sigma}_{min}$ for both types of connections are shown in Figs. 10 and 11. The statistics are presented in Table 3. The coefficients of variation are close for the investigated quantities of interest: 24% for $\overline{\sigma}_{max}$ and $\overline{\sigma}_{min}$ of the dovetail connection and 23% for $\overline{\sigma}_{max}$ and $\overline{\sigma}_{min}$ of saddle notch joint. The distribution of $\overline{\sigma}_{min}$ is similar for both connections. More significant differences between connections can be noted for $\overline{\sigma}_{max}$, of which the mean and 95th percentile is higher in case of saddle notch than in the short-corner dovetail.

Table 4 presents the total sensitivity indices obtained by the third order PC. Although the assumed coefficient of variation of μ is higher than of E_L, sensitivity indices of E_L (S_1^{tot}) are for all quantities of interest much higher than of μ (S_2^{tot}). The sensitivity indices obtained for two connections mostly differ in the case of the quantities of interest related to the maximum principal stress. The value of $\overline{\sigma}_{max}$ is more sensitive on the variation of μ for the short-corner dovetail connection than for the saddle notch. However this sensitivity is still low. The value of S_2^{tot} is relatively high when compared to the other quantities of interest, only in the case of $\max\sigma_{max}$ in the model of the short dovetail connection. In the majority of cases the uncertainty of μ shows a negligible effect on the variation of investigated quantities of interest. According to [32,42,49] the friction coefficient plays the leading role in the mechanical behaviour of some carpentry joints. But in the case of considered joints and quantities of interest, the mean principal stress in
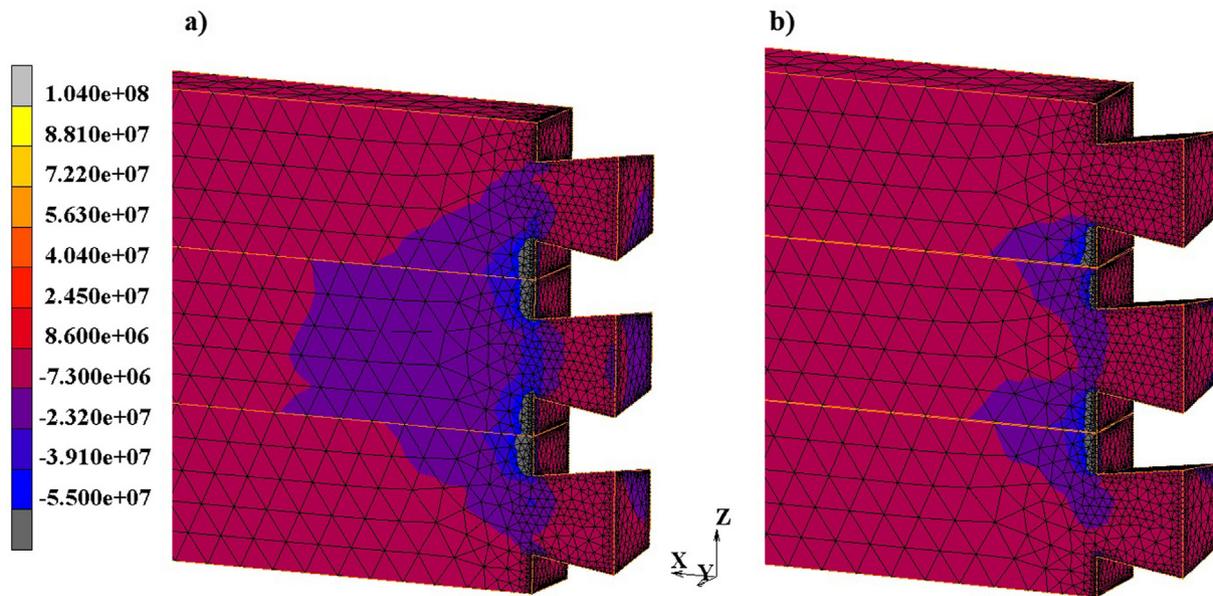
Fig. 6. Distribution of minimum principal stress [Pa] in the corner of short-corner dovetail connection for: (a) variant A, (b) variant B.
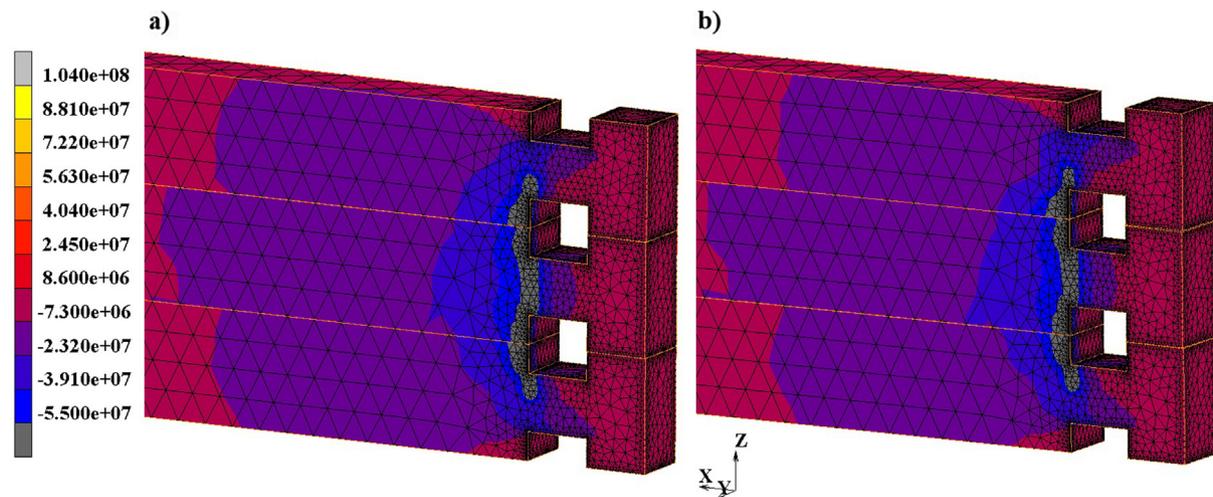

Fig. 7. Distribution of minimum principal stress [Pa] in the corner of saddle notch for: (a) variant A, (b) variant B.
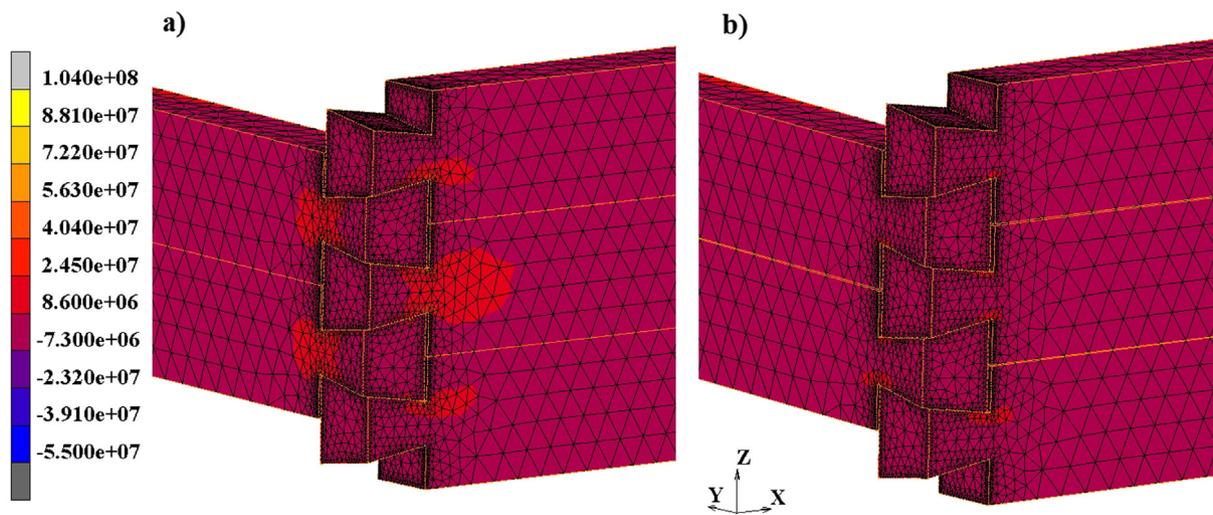

Fig. 8. Distribution of maximum principal stress [Pa] in the corner of short-corner dovetail connection for: (a) variant A, (b) variant B.
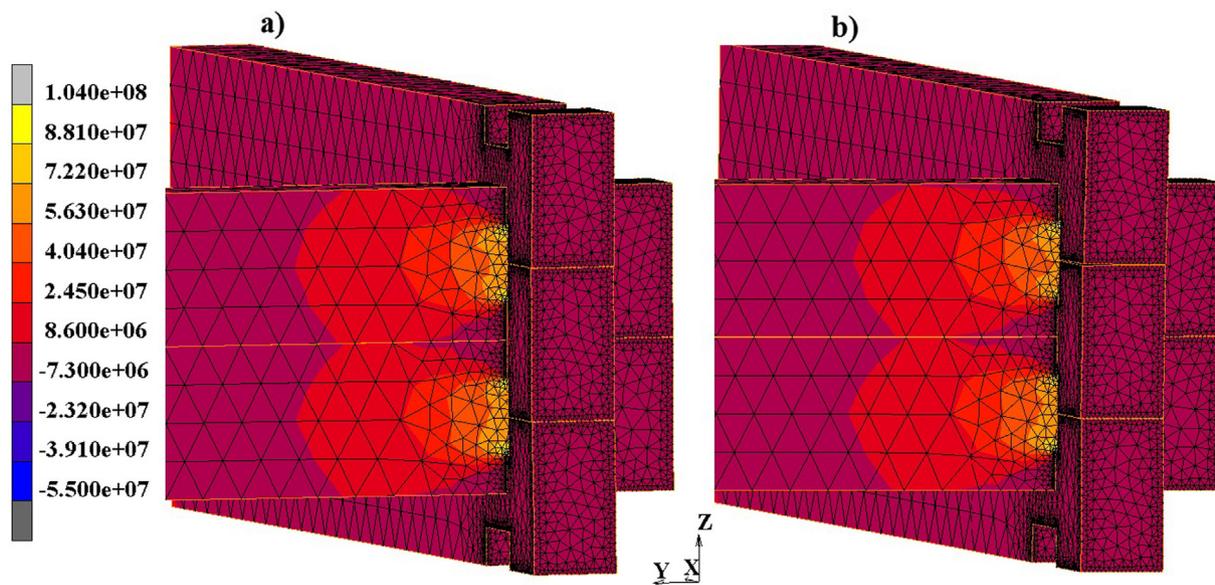
Fig. 9. Distribution of maximum principal stress [Pa] in the corner of saddle notch for: (a) variant A, (b) variant B.
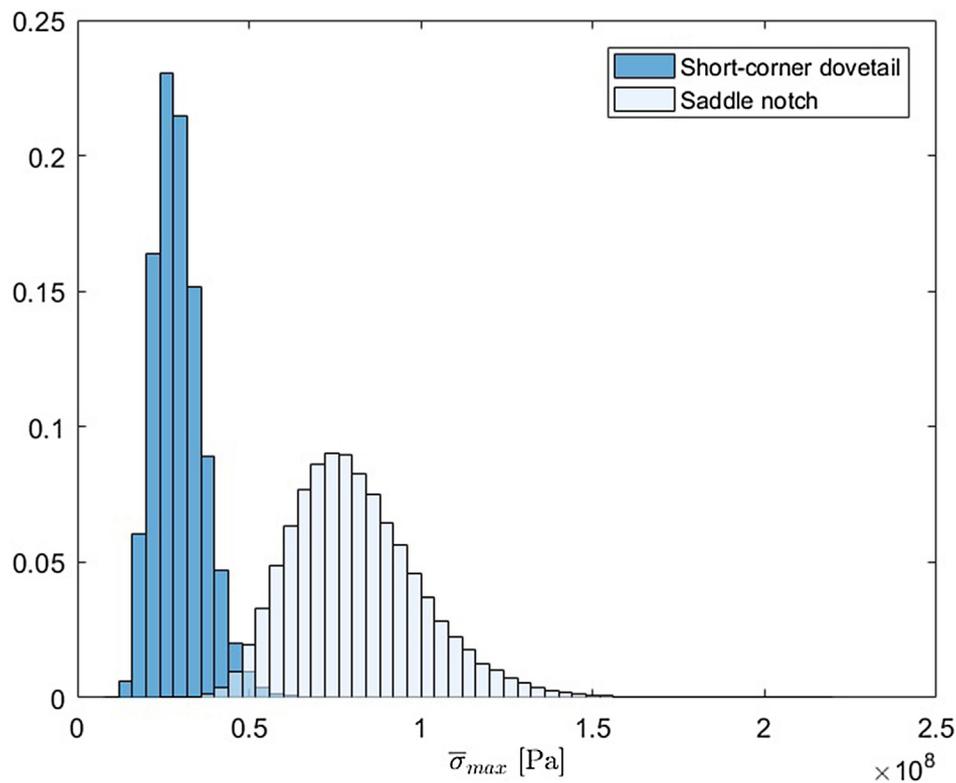

Fig. 10. Normalized histograms of $\overline{\sigma}_{max}$ [Pa] obtained for both connection types.

chosen elements in the high stress zone, the effect of μ uncertainty is negligible when compared to the influence of the uncertainty of E_L. Therefore, the identification of the friction coefficient distribution in a given system is not a priority in the case of investigated connections and considered quantities. Thus the attention should be focused on the identification of the material properties.

4. Conclusions

Two types of carpentry joints commonly used in the currently preserved structures of wooden architecture have been analysed with the two variants of boundary conditions and load schemes.

The highest stress areas have been detected on the basis of the numerical analysis since the analysed carpentry joints are prone to be damaged in obtained places with the greatest stress areas. Comparing the stress value and distribution in saddle notch joint and the dovetail connection one could say that the first one is more susceptible to damage but, on the other hand, owing to its geometry is more hermetic, so less sensitive to moisture penetration. Dovetail joint is less hermetic, so that more disposed to biological corrosion but it supports higher force so it is more damage resistant. Only local damage (potential plastic deformation) can be observed in the highest stress zones. During loading of the dovetail connection the logs are disassembling, so potentially can be assembled again.
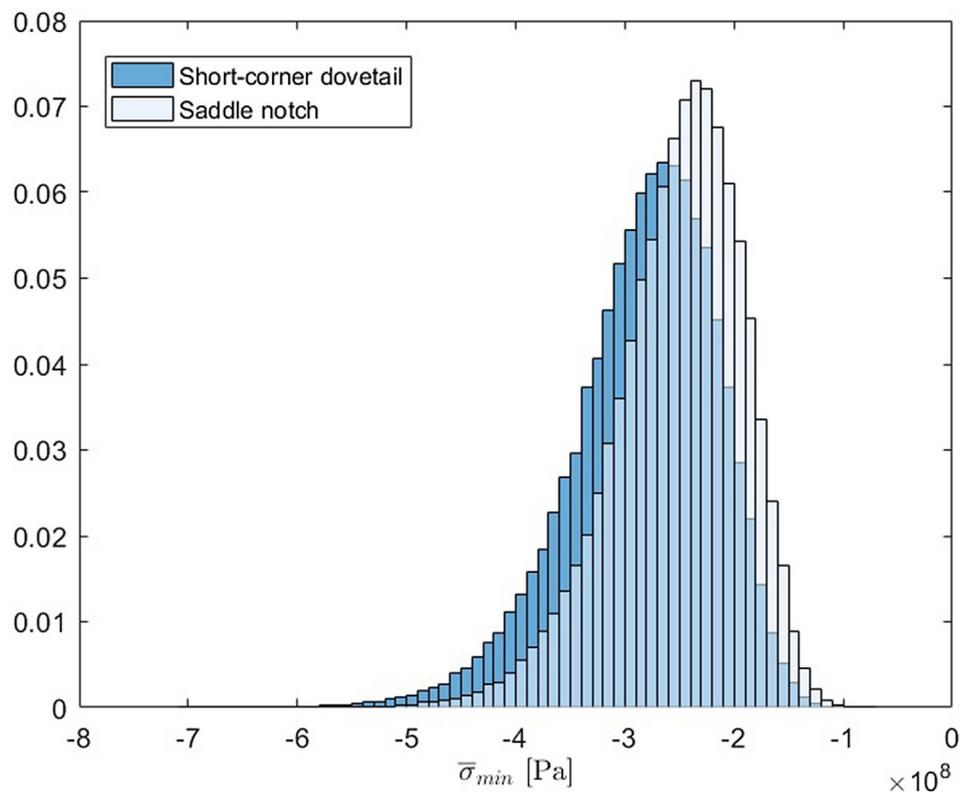
Fig. 11. Normalized histograms of $\overline{\sigma}_{min}$ [Pa] in the case of both connection types.

Table 3
Statistic of the outcome [Pa].

Type of connection	Short-corner dovetail		Saddle notch	
Quantity of interest	$\overline{\sigma}_{max}$	$\overline{\sigma}_{min}$	$\overline{\sigma}_{max}$	$\overline{\sigma}_{min}$
Mean	2.95E+07	−2.83E+08	8.12E+07	−2.52E+08
Standard deviation	7.16E+06	6.70E+07	1.90E+07	5.91E+07
5th percentile	1.93E+07	−4.05E+08	5.40E+07	−3.59E+08
95th percentile	4.25E+07	−1.88E+08	1.16E+08	−1.67E+08

In the case of the saddle notch joint the stress distribution in the connection corner for the variants A and B is almost identical. Thus, the stress distribution is not strongly related to the boundary conditions. This is effected by the shape of the carpentry joint or the inability to deform significantly like in the case of the dovetail connections. In turn, differences are observed in the dovetail connection between the stress distribution in the variants A and B. The obtained results for the variant B are more realistic due to the fact that under the influence of atmospheric conditions the wood desiccates and swells, thus there is a possibility of motion in the direction Z.

The uncertainty propagation of the Young's modulus and the friction coefficient has been introduced in the model of the connections. The variation of the mean of the principal stress in elements located in high stress zone is high, 23–24%. The effect of the uncertainty of the friction coefficient is negligible, whereas the influence of uncertainty of

the Young's modulus is dominating on the variance of the mean principal stress. Although we considered variability of the material properties amongst only one kind of wood (pinewood), the variance of the output due to variance of Young's modulus is high. Therefore, it can be seen that uncertainty quantification is needed even when the kind of wood is known. Incorporating variability amongst different kinds of wood would probably lead to even higher variance of output. The conducted global sensitivity analysis may be the basis for effective planning of further experimental research where special attention should be paid to material testing of the wood used for construction of joints to be compared. The presented probabilistic approach gives significant results even in a fairly classical problem, which testifies to the novelty of the presented research.

Some limitation of the presented study should be pointed out. First, only elastic material model was assumed in the analysis. Second limitation is the uncertainty of input distribution and assumption of full correlation of E_L with other parameters of the orthotropic material model. Negligibly small value of total sensitivity index of friction coefficient indicates that more detailed studies of its distributions are not as important as studies on material parameters of wood. The model could also be reduced where the friction coefficient would not be treated as a random variable. More attention should be paid to the material parameters. In the future research the material parameters will not be fully correlated and random fields will be applied in order to include spatial variability.

Table 4
Sobol' total indices for considered quantities of interest.

	Short-corner dovetail				Saddle notch			
	$\overline{\sigma}_{max}$	$\overline{\sigma}_{min}$	$\max\sigma_{max}$	$\min\sigma_{min}$	$\overline{\sigma}_{max}$	$\overline{\sigma}_{min}$	$\max\sigma_{max}$	$\min\sigma_{min}$
S_1^{Tot}	0.937	0.9851	0.7101	0.9931	0.9998	0.9886	0.9859	0.999
S_2^{Tot}	0.0641	0.0156	0.3104	0.0075	0.0003	0.0119	0.0151	0.0011

Acknowledgment

Appendix A. Supplementary material

Supplementary data associated with this article can be found, in the online version, at https://doi.org/10.1016/j.engstruct.2018.08.095.

References

[1] Green DW, Winandy JE, Kretschmann DE. Wood handbook—wood as an engineering material. Madison; 1999.

[2] Nowak TP, Jasieńko J, Hamrol-Bielecka K. In situ assessment of structural timber using the resistance drilling method—evaluation of usefulness. Constr Build Mater 2016;102:403–15.

[3] Michniewicz W. Konstrukcje drewniane (Wooden construction). Arkady, Warsaw; 1958.

[4] Sonderegger W, Kránitz K, Bues C-T, Niemz P. Aging effects on physical and mechanical properties of spruce, fir and oak wood. J Cult Heritage 2015;16(6):883–9.

[5] Morales-Conde MJ, Machado JS. Evaluation of cross-sectional variation of timber bending modulus of elasticity by stress waves. Constr Build Mater 2017;134:617–25.

[6] Jasieńko J, Nowak T, Karolak A. Historyczne złącza ciesielskie (Historical carpentry joints). J Heritage Conserv 2014;40:58–82.

[7] Sangree RH, Schafer B. Experimental and numerical analysis of a halved and tabled traditional timber scarf joint. Constr Build Mater 2009;23(2):615–24.

[8] Aira J, Íñiguez-González G, Guaita M, Arriaga F. Load carrying capacity of halved and tabled tenoned timber scarf joint. Mater Struct 2016;49(12):5343–55.

[9] Palma P, Garcia H, Ferreira J, Appleton J, Cruz H. Behaviour and repair of carpentry connections—rotational behaviour of the rafter and tie beam connection in timber roof structures. J Cult Heritage 2012;13(3):S64–73.

[10] Jasieńko J, Engel L, Rapp P. Study of stresses in historical carpentry joints by photoelasticity modelling. In: Lourenço editor. Structural analysis of historical constructions, possibilities of numerical and experimental techniques. New Delhi: Macmillan India Ltd.; 2006.

[11] Jasieńko J, Kardysz M. Deformation and strength criteria in assessing mechanical behaviour of joints in historic timber structures. In: Proceedings of the 16th international conference: from material to structure – mechanical behaviour and failures of the timber structures. ICOMOS international wood committee, no; November, 2007. p. 218–30.

[12] Rajczyk M, Jończyk D. Analiza numeryczna belki drewnianej (Numerical analysis of timber beam). Sci Pap Czestochowa Univ Technol 2014;20:231–9.

[13] Trochonowicz M, Kołodziejczuk N. Wpływ temperatury, wilgotności i kierunku badań na wartość współczynnika przewodności cieplnej λ w różnych gatunkach drewna (The impact of temperature, humidity and the direction of analysis on thermal conductivity λ in different types of wood). Budownictwo i Architektura 2015;14(4):149–56.

[14] Kozakiewicz P. Effects of temperature and humidity on the compressive strength along fibres selected types of wood of varying density and anatomical structure. Warsaw: SGGW Publisher; 2010.

[15] Villar J, Guaita M, Vidal P, Arriaga F. Analysis of the stress state at the cogging joint in timber structures. Biosyst Eng 2007;96(1):79–90.

[16] Schmidt J, Kaliske M. Models for numerical failure analysis of wooden structures. Eng Struct 2009;31(2):571–9.

[17] Calderoni C, De Matteis G, Giubileo C, Mazzolani F. Experimental correlations between destructive and non-destructive tests on ancient timber elements. Eng Struct 2010;32(2):442–8.

[18] Calderoni C, De Matteis G, Giubileo C, Mazzolani F. Flexural and shear behaviour of ancient wooden beams: experimental and theoretical evaluation. Eng Struct 2006;28(5):729–44.

[19] Armesto J, Lubowiecka I, Ordóñez C, Rial FI. FEM modeling of structures based on close range digital photogrammetry. Automat Constr 2009;18(5):559–69.

[20] Humbert J, Boudaud C, Baroth J, Hameury S, Daudeville L. Joints and wood shear walls modelling I: constitutive law, experimental tests and FE model under quasi-static loading. Eng Struct 2014;65:52–61.

[21] Boudaud C, Humbert J, Baroth J, Hameury S, Daudeville L. Joints and wood shear walls modelling II: experimental tests and FE models under seismic loading. Eng Struct 2015;101:743–9.

[22] Sørensen JD. Framework for robustness assessment of timber structures. Eng Struct 2011;33(11):3087–92.

[23] Lourenço PB, Sousa HS, Brites RD, Neves LC. In situ measured cross section geometry of old timber structures and its influence on structural safety. Mater Struct 2013;46(7):1193–208.

[24] Brites RD, Neves LC, Machado JS, Lourenço PB, Sousa HS. Reliability analysis of a timber truss system subjected to decay. Eng Struct 2013;46:184–92.

[25] Stefanou G. The stochastic finite element method: past, present and future. Comput Methods Appl Mech Eng 2009;198(9–12):1031–51.

[26] Kandler G, Füssl J. A probabilistic approach for the linear behaviour of glued laminated timber. Eng Struct 2017;148:673–85.

[27] Sobol IM. Global sensitivity indices for nonlinear mathematical models and their Monte Carlo estimates. Math Comput Simul 2001;55(1–3):271–80.

[28] Hristov P, DiazDelaO F, Flores ES, Guzmán C, Farooq U. Probabilistic sensitivity analysis to understand the influence of micromechanical properties of wood on its macroscopic response. Compos Struct 2017;181:229–39.

[29] Klein A, Grabner M. Analysis of construction timber in rural Austria: wooden log walls. Int J Archit Heritage 2015;9(5):553–63.

[30] Mleczek A, Kłosowski P. Numerical analysis of the carpentry joints applied in the traditional wooden structures. In: Advances in mechanics: theoretical, computational and interdisciplinary issues: proceedings of the 3rd polish congress of mechanics (PCM) and 21st international conference on computer methods in mechanics (CMM), Gdansk, Poland, 8–11 September 2015. CRC Press; 2016. p. 409.

[31] Bedon C, Rinaldin G, Fragiacomo M. Non-linear modelling of the in-plane seismic behaviour of timber Blockhaus log-walls. Eng Struct 2015;91:112–24.

[32] Grossi P, Sartori T, Giongo I, Tomasi R. Analysis of timber log-house construction system via experimental testing and analytical modelling. Constr Build Mater 2016;102:1127–44.

[33] Nowak TP, Jasieńko J, Czepiżak D. Experimental tests and numerical analysis of historic bent timber elements reinforced with CFRP strips. Constr Build Mater 2013;40:197–206.

[34] Phleps H. Holzbaukunst de Blockbau, Karlsruhe; 1942.

[35] Cielątkowska R. Translocatio. Przeniesienie drewnianych świątyń trzech obrządków (Translocatio Transfer of wooden temples of the three religions). Gdańsk: Department of Architecture of Gdansk University of Technology; 2014.

[36] Berveiller M, Sudret B, Lemaire M. Stochastic finite element: a non intrusive approach by regression. Eur J Comput Mech/Revue Européenne de Mécanique Numérique 2006;15(1–3):81–92.

[37] Kopkowicz F. Ciesielstwo polskie (Polish carpentry). Arkady, Warsaw; 1958.

[38] Kyzioł L. Zastępcze stałe materiałowe drewna konstrukcyjnego modyfikowanego powierzchniowo PMM (Substitute material parameters of structural wood with surface modification PMM). In: Scientific papers of Polish Naval Academy, vol. 1, Gdynia; 2005. p. 69–82.

[39] JCSS. Probabilistic Model. Joint committee on structural safety. < www.jcss. ethz.ch > .

[40] Blau PJ. The significance and use of the friction coefficient. Tribol Int 2001;34(9):585–91.

[41] McKenzie W, Karpovich H. The frictional behaviour of wood. Wood Sci Technol 1968;2(2):139–52.

[42] Parisi MA, Piazza M. Mechanics of plain and retrofitted traditional timber connections. J Struct Eng 2000;126(12):1395–403.

[43] Xu M, Li L, Wang M, Luo B. Effects of surface roughness and wood grain on the friction coefficient of wooden materials for wood–wood frictional pair. Tribol Trans 2014;57(5):871–8.

[44] Blatman G, Sudret B. Efficient computation of global sensitivity indices using sparse polynomial chaos expansions. Reliab Eng Syst Saf 2010;95(11):1216–29.

[45] Zein S, Colson B, Glineur F. An efficient sampling method for regression-based polynomial chaos expansion. Commun Comput Phys 2013;13(4):1173–88.

[46] Szepietowska K, Magnain B, Lubowiecka I, Florentin E. Sensitivity analysis based on non-intrusive regression-based polynomial chaos expansion for surgical mesh modelling. Struct Multidiscipl Optimiz 2018;57(3):1391–409.

[47] Sudret B. Global sensitivity analysis using polynomial chaos expansions. Reliab Eng Syst Saf 2008;93(7):964–79.

[48] Crestaux T, Le Maître O, Martinez J-M. Polynomial chaos expansion for sensitivity analysis. Reliab Eng Syst Saf 2009;94(7):1161–72.

[49] Parisi MA, Cordié C. Mechanical behavior of double-step timber joints. Constr Build Mater 2010;24(8):1364–71.